4

Imaging Laser Absorption Spectroscopy of the metal-halide lamp in a centrifuge (1–10g)

Abstract.
Imaging Laser Absorption Spectroscopy (ILAS) was performed on a metal-halide lamp under hyper-gravity conditions in a centrifuge (acceleration ranging from 1 to 10g). Diffusive and convective processes in the arc discharge lamp cause an unwanted non-uniform distribution of the radiating metal additive, which results in colour separation. Convection is induced by gravity, and measuring under different apparent gravity conditions aids the understanding of the flow processes in the lamp. The centrifuge was built to investigate the lamp under varying apparent gravity conditions. The metal additive density distribution in the lamp is measured by ILAS. In this novel diagnostic technique the laser beam is expanded, so the absorption in the complete plasma volume is imaged simultaneously.
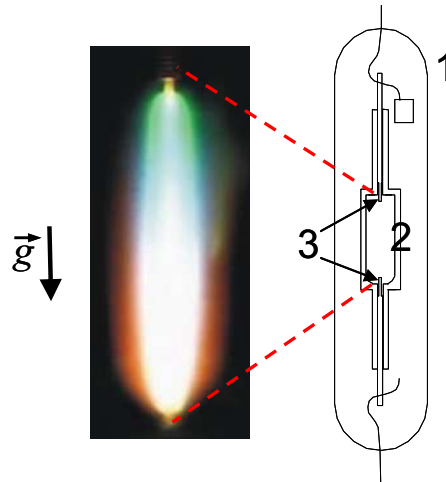
Figure 4.1: (printed in colour in figure 1.3) Left: picture of the burner of a MH lamp (real size 8 mm x 20 mm; filling 10 mg Hg and 4 mg DyI_3); colour separation is clearly visible. The exponential decay of the radiating particle (white) towards the top has a maximum when the convection and diffusion are of the same order of magnitude. Right: schematic picture of the lamp, (1) outer bulb; (2) burner with height 20 mm and diameter 8 mm; (3) electrodes, distance between both electrodes ∼18 mm.

4.1   Introduction

Many plasmas have an axis of symmetry. They are cylindrical symmetric but inhomogeneous in the axial direction. A useful diagnostic tool to investigate these plasmas is Imaging Laser Absorption Spectroscopy (ILAS). Laser absorption spectroscopy has been used in earlier experiments (chapters 2 and 3) to measure the particle density distribution in a plasma [32, 33]. However, in order to image the absorption in the complete plasma volume simultaneously (2D), in the novel ILAS setup laser beam expansion is used, so every part of the laser beam samples a different part of the plasma. This chapter outlines this new technique of laser absorption spectroscopy.

The novel ILAS technique is applied on a metal-halide (MH) lamp. This lamp is a compact high-intensity light source with a high luminous efficacy and a good colour rendering index. It has a high efficiency (up to 40%) compared with present (compact) fluorescent lamps [3, 21–26]. The arc discharge lamp contains a buffer gas (mercury) and (a combination of) metal additives (for instance Na, Ce, Dy), which are dosed as metal-halide salts. After ignition of the lamp, the salt evaporates and enters the arc. The metal additives act as the prime radiator in the visible spectrum. The local density distribution of the additive is determined by convective and diffusive processes,
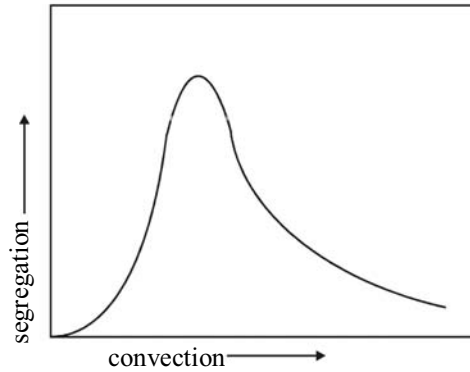
Figure 4.2: The Fischer curve [28, 33]: axial segregation (λ) of the metal additive in an infinitely long lamp as a function of the amount of convection. Convection is induced by gravity. In our experiment, the amount of convection is increased by increasing the gravity.

which cause an unwanted non-uniform distribution of the additives in the lamp. The processes result in a segregation of colours [27, 28, 32–34, 38, 41]: so-called demixing. The colour separation and a schematic picture of the lamp are shown in figure 4.1.

The large temperature gradient between the wall ($\sim$1200 K) and the centre of the burner ($\sim$5500 K) [29] leads to the situation that atoms are mainly present at the centre while molecules dominate at the wall. In addition, the metal atoms are partially ionized at the very centre of the burner because of the high temperature. The diffusion velocities of atoms, molecules and ions (ambipolar diffusion) are different. The light particles at the hot centre diffuse outwards faster than the heavy molecules near the cooler wall diffuse inwards. This difference in diffusion times results in a hollow radial profile of the elemental metal relative concentration (the metal additive in any chemical form) in addition to the already lower gas density defined by the ideal gas law $p = nkT$; this mechanism is called radial segregation. Due to radial segregation, the maximum of the elemental metal relative concentration lies near the wall. The second mechanism, convection, causes the hot gas at the centre to move upwards, whereas the gas near the cooler wall moves downwards. The combination of radial segregation and convection results in a net downward transport of the metal additive which is balanced by an axial density gradient: the so-called axial segregation [21, 22, 32].

When the convective and diffusive processes are of the same order of magnitude, axial segregation of the metal additive occurs because of the competition between these two processes. In the two limiting cases, when there is no convection, or when there is extremely high convection, good mixing and thus no axial segregation is achieved (figure 4.2).

Because the convection is induced by gravity, the lamp was investigated at microgravity in the International Space Station (ISS) [41] and at micro-gravity and hyper-gravity ($\sim 1.8g$) during parabolic flights [33, 43, 51, 52]. Measuring under different gravity conditions aids the understanding of the diffusive and convective processes. However, during the parabolic flights micro-gravity and hyper-gravity were obtained for a period of only about 20 s. This is not enough time for the arc to stabilize. A centrifuge was built for this purpose: to investigate the lamp in an environment where stable arc conditions are ensured. The centrifuge can go up to $10g$, thus the lamp can be investigated under even higher gravity conditions than during the parabolic flights. The measurement techniques used in the centrifuge are emission spectroscopy and ILAS.

The structure of this chapter is as follows. Section 4.2 describes the centrifuge. The diagnostics are described in section 4.3. Section 4.4 presents some first results of the ILAS measurements on the lamp in the centrifuge. Finally, section 4.5 gives conclusions and some recommendations for future work.

4.2 The centrifuge

A centrifuge was built as a tool to investigate the MH lamp [27] under hyper-gravity conditions up to $10g$. The centrifuge consists of a pivot, an arm connected to the pivot and at the end of the arm a gondola, in which the lamp is placed. Furthermore, the gondola contains the measurement techniques and electronics. In figure 4.3 the schematic representation of the centrifuge is shown; the coordinate system of the lamp in the gondola is indicated ($\vec{z}$ is parallel to the lamp axis). The total diameter at maximum swing-out of the gondola is close to 3 m; the maximum rotation frequency is ~ 1.5 Hz. Figure 4.4 shows the dimensions of the centrifuge and the acceleration vectors at the position of the lamp.

4.2.1 Acceleration

The total acceleration vector experienced by the lamp depends on the rotation frequency of the centrifuge. When the rotation frequency increases, the distance between the lamp and the axis of the centrifuge increases. When this is taken into account, the size of the centrifugal acceleration vector $\vec{a}_r$ (figure 4.4) is given by

$$a_r = \omega^2 \cdot (r_1 + r_2 \sin \phi).$$
(4.1)

Here ω is the angular frequency of the centrifuge, r_1 is the arm length of the centrifuge, r_2 is the distance between the gondola hinge point and the centre of the lamp and ϕ is the angle of swing-out of the gondola. Using the relation for the magnitude of the resultant acceleration vector

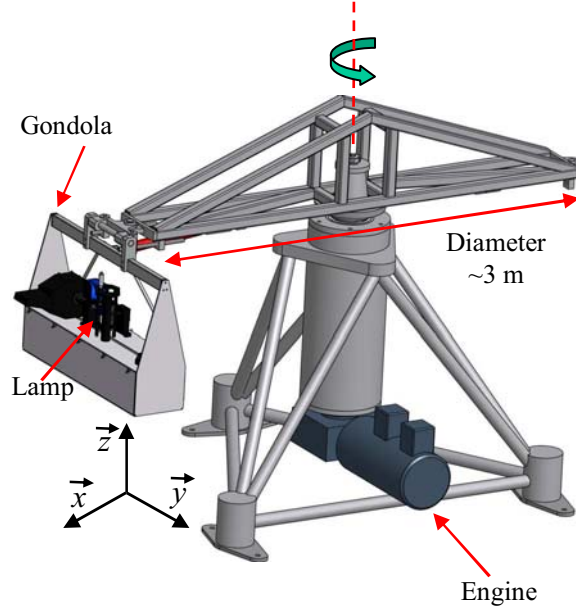$$a_{\text{tot}} = \sqrt{a_r^2 + g_z^2},$$
(4.2)

Figure 4.3: Schematic representation of the centrifuge. The setup consists of a pivot, an arm and the gondola that contains the lamp and diagnostic equipment (figures 4.8 and 4.11). The coordinate system shown is that of the lamp in the gondola; $\vec{z}$ is parallel to the lamp axis.

where g_z is the magnitude of the gravity on earth, one gets the following relation:

$$a_{\text{tot}}^2 - g_z^2 = \omega^4 \cdot \left(r_1 + \frac{r_2}{a_{\text{tot}}} \sqrt{a_{\text{tot}}^2 - g_z^2} \right)^2 . \tag{4.3}$$

Ideally $\vec{a}_{\text{tot}}$ is parallel to the lamp axis. Therefore it is necessary that the centre point of mass of the gondola is located along the axis of the lamp. The resultant acceleration vector always acts in the right direction when the gondola swings radially outwards. Looking at figure 4.4, this means that $a_{\text{tot}} = a_z$ ($\vec{a}_z$ is parallel to the lamp axis) and thus $a_x = a_y = 0$. The vector $\vec{a}_x$ is along the optical path and $\vec{a}_y$ is perpendicular to $\vec{a}_x$ and $\vec{a}_z$. To verify the direction of the acceleration vector $\vec{a}_{\text{tot}}$, the lamp is substituted by an accelerometer (Endevco 7596A-30). The sizes of the three vectors $\vec{a}_x$, $\vec{a}_y$ and $\vec{a}_z$ are measured as functions of the rotation frequency of the centrifuge $f = \omega/2\pi$. The calibration curve for $\vec{a}_z$ is shown in figure 4.5. Figure 4.6 shows the curves for $\vec{a}_x$ and $\vec{a}_y$. In these figures the unit G is defined as 9.81 m s^{-2}. The accelerations in $\vec{x}$ and $\vec{y}$ direction are less than 0.13 G and 0.07 G, respectively. The maximum ratios between the accelerations in the $\vec{x}$ and $\vec{y}$ directions and the acceleration
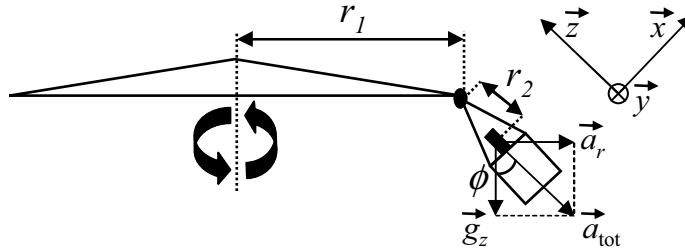
Figure 4.4: Schematic representation of the centrifuge arm with gondola. The dimensions are $r_1 = 1.0975$ m and $r_2 = 0.3485$ m. When the centrifuge is rotating, the gondola swings out with an angle ϕ. The acceleration vectors at the position of the lamp ($\vec{g}_z$, $\vec{a}_r$, $\vec{a}_{\text{tot}}$) are indicated; the coordinate system relative to the lamp (from figure 4.3) is also indicated.
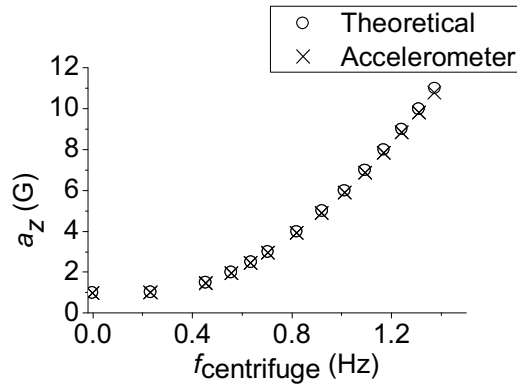

Figure 4.5: Theoretical (equation (4.3)) and measured acceleration at the position of the lamp. The acceleration a_z is measured parallel to the lamp axis, as a function of the centrifuge rotation frequency.

a_z are less than 5% below $5g$. At $10g$ the accelerations in the $\vec{x}$ and $\vec{y}$ directions are less than 1%. A slight variation in the acceleration occurs along the lamp axis, because the top of the lamp is closer to the centre point of the centrifuge. However, this is only a variation of 0.7% and is therefore not taken into account. Calibration with an accelerometer thus shows that the acceleration vector that acts on the lamp is always parallel to the lamp axis.
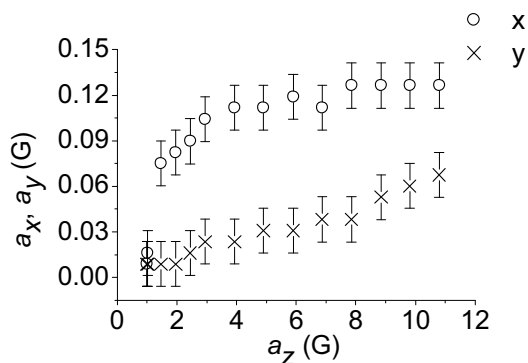
Figure 4.6: Accelerations a_x and a_y (perpendicular to the lamp axis) as a function of a_z (parallel to the lamp axis), measured at the lamp axis. The error bars show the inaccuracy of the accelerometer. Ideally the acceleration is parallel to the lamp axis and the accelerations perpendicular to the lamp axis should be zero.

4.2.2 Gondola

A gondola is attached to the end of the arm of the centrifuge. The gondola contains the setup that consists of the lamp, the electronics and the measurement techniques. A mini-computer in the gondola is used to control the lamp power and to perform the acquisition. The data from the measurements are stored locally. To improve the performance of the measurement technique, the data are transferred via the network only after the measurements have been finished.

On top of the gondola two interchangeable setups can be placed, one for emission spectroscopy and one for ILAS. Both setups contain the lamp and a webcam to monitor the lamp. Webcam images show the effect of hyper-gravity on the lamp in the centrifuge. Some webcam images of the lamp containing 5 mg of mercury are shown in figure 4.7. This figure shows that the axial segregation is strongly reduced at 10g.

4.3 Diagnostics

The two measurement techniques used to investigate the lamp, emission spectroscopy and ILAS, will be discussed in turn.

4.3.1 Emission spectroscopy

The lamp is investigated using absolute line intensity spectroscopy, yielding the laterally resolved spectrum. After the calibration of intensity and wavelength, absolute radial density distributions of several particles in excited states are obtained. Furthermore,
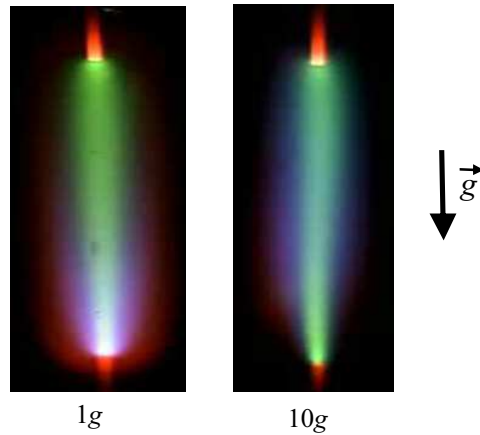
Figure 4.7: Webcam pictures of the lamp containing 4.2 mg DyI$_3$ and 5 mg Hg in the centrifuge [38], at 1g and 10g. The input power is 130 W. Colour separation is seen at 1g; at 10g the convection is dominant over diffusion and the colour separation disappears: the bluish-white light caused by the Dy atoms is more evenly distributed over the lamp.

several plasma properties can be determined, such as the temperature distribution, the ground state densities and the electron density.

Densities and plasma properties of the lamp have been measured by emission spectroscopy in experiments done previously [34, 41]. The setup used in these experiments is adjusted so it fits on top of the gondola for use in the centrifuge. In figure 4.8 a schematic overview of the emission spectroscopy setup is shown. An example of a lateral (line-of-sight) atomic dysprosium profile is shown in figure 4.9; the data are taken near the top of the lamp. Other results obtained by emission spectroscopy in the centrifuge are discussed by Nimalasuriya *et al* [38].

4.3.2 Imaging Laser Absorption Spectroscopy

The second measurement technique used in the centrifuge, ILAS, is a novel technique, with which the 2D density distribution of the radiating particles can be obtained. The theory of laser absorption spectroscopy has been described in chapters 2 and 3 [32, 33]. For clarity, the principles are summarized here.

General

In our experiment ILAS is used to obtain a 2D atomic density distribution of the metal additive in the lamp burner. A laser beam is expanded so that it illuminates the full lamp burner. When the lamp is switched on, part of the laser light is absorbed by the
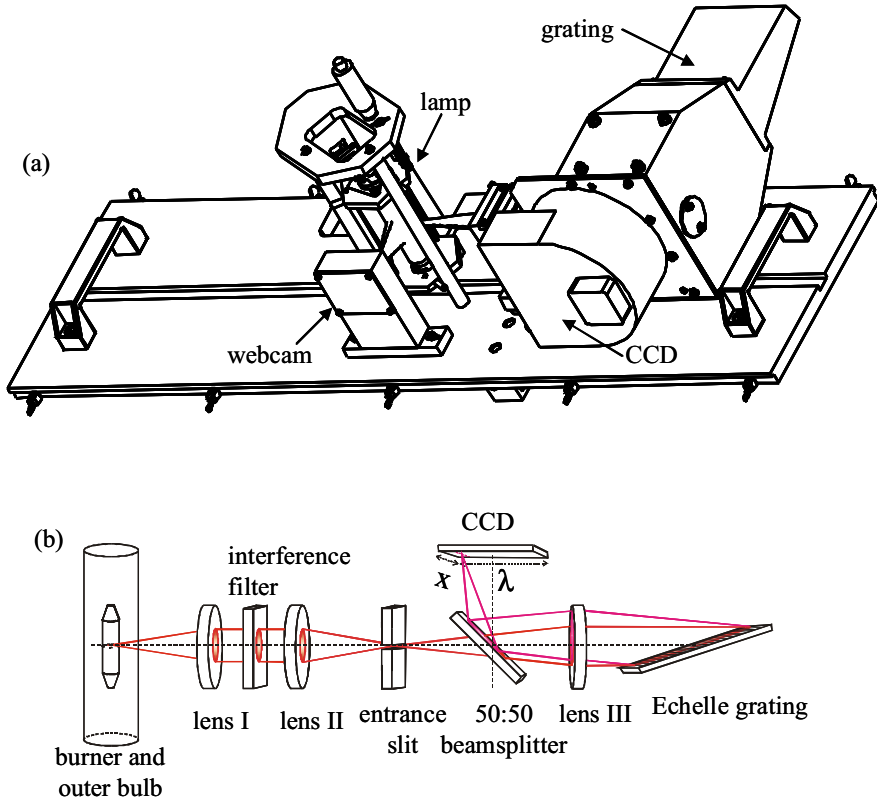
Figure 4.8: (a) Schematic drawing of the emission spectroscopy setup for the centrifuge. (b) Artist impression of the Echelle type spectrometer used in the ISS [38, 41]. In the centrifuge the beam splitter, CCD and the grating + lens III are rotated by 90° as is showed in (a).

metal additive particles. Behind the lamp, a CCD camera detects the light that passes through the lamp burner. The tunable diode laser (Sacher TEC 500 645-5) scans step by step over a wavelength range around an absorption line of the particle. At each wavelength step an image is taken by the CCD camera. The local line-of-sight atomic density n_{los} for each pixel on the CCD camera, which corresponds to a unique position in the lamp burner, is given by [32, 43–45, 47]:

$$n_{\mathrm{los}} = -\frac{c}{S\lambda^2} \int \ln\left(T_\lambda\right) \mathrm{d}\lambda, \tag{4.4}$$
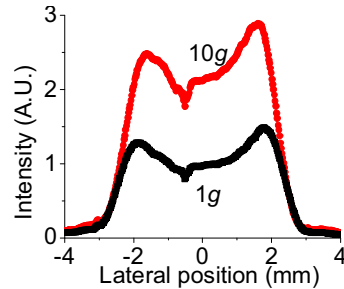
Figure 4.9: Atomic lateral profile of the atomic Dy line at 642.19 nm, measured by means of emission spectroscopy [38]. The lamp contains 4.2 mg DyI$_3$ and 5 mg Hg. The lamp input power is 150 W. The measurement is taken near the top of the burner ($y = 13$ mm; electrode distance in the burner is 18 mm). The intensity near the top of the lamp is higher at $10g$ than $1g$. The jump that is observed around -1 mm at $10g$ is due to a small imperfection of the slit in the spectrometer.

where c is the speed of light, S is the line strength of the transition, T_λ is the transmission (laser intensity at the CCD with absorption divided by the intensity without absorption) at wavelength λ. The integral is taken over the line width of the absorption line.

Measurement procedure

ILAS is used in our experiment to obtain the line-of-sight ground state atomic dysprosium density distribution in the lamp burner. In this section we discuss the necessary steps to obtain this density. During all these steps the lamp is turned on. The measurement by the CCD camera (SBIG ST-2000XM with 1600×1200 pixels of 7.4 μm $\times$ 7.4 μm [60]) consists of a dark current measurement (shutter closed), a lamp emission measurement I_e, a reference measurement I_0 and the actual measurement I_λ: the scanning by the laser around the absorption wavelength.

The first two measurements are the dark current and lamp emission images. The next measurement is the reference measurement. The wavelength of the laser is chosen just outside the absorption dip, where no absorption takes place. Next, the actual absorption measurement starts. A tunable laser scans over a wavelength range of $\sim$0.1 nm around the absorption wavelength of $\lambda = 642.19$ nm in N steps (in our experiments $N = 65$).

Data processing is as follows. First, dark current and lamp emission correction are applied to the reference and absorption images. Second, for each wavelength step n a relative transmission image is constructed by dividing the corrected absorption image

by the corrected reference image. The transmission is given by

$$T_\lambda = \frac{(I_\lambda - I_{\mathrm{d},\lambda}) - (I_\mathrm{e} - I_{\mathrm{d,e}})}{(I_0 - I_{\mathrm{d},0}) - (I_\mathrm{e} - I_{\mathrm{d,e}})} \times \frac{I_{\mathrm{ph},0}}{I_{\mathrm{ph},\lambda}}, \tag{4.5}$$

where $I_{\mathrm{d,e}}$, $I_{\mathrm{d},0}$ and $I_{\mathrm{d},\lambda}$ are the darkcurrents in the emission, reference and measurements, respectively, and $I_{\mathrm{ph},0}$ and $I_{\mathrm{ph},\lambda}$ are the integrated laser intensities (measured by a photodiode) before entering the plasma for the reference and absorption measurements, respectively. This intensity correction is explained in section 4.3.2.

We thus obtain a 3D matrix filled with relative transmission values T; so we get $T(\lambda(n), x, y)$: n is the wavelength step, x and y are the positions on the CCD camera. From this matrix, for each (x, y) equation (4.4) is used to calculate the line-of-sight atomic density n_{los}:

$$n_{\mathrm{los}}(x, y) = -\frac{c}{S\lambda^2} \int \ln T(\lambda(n), x, y) \mathrm{d}\lambda. \tag{4.6}$$

The integral is evaluated by fitting the area under the $\ln T$ curve.[1] Finally, a 2D ground state atomic Dy density distribution image is constructed from all these line-of-sight densities.

Figure 4.10 shows how the absorption curves for each pixel (x,y) of the CCD camera are constructed and an example of the relative transmission curve for an arbitrary pixel of the CCD; the reference measurement and the absorption measurements are indicated in the figure.

Setup

The ILAS setup in the centrifuge is shown in figure 4.11. Some problems were encountered during development of the ILAS technique. In contrast to the earlier laser absorption setup in chapters 2 and 3 [32, 33], the whole lamp burner is illuminated by the laser using beam expansion. Each point in the illuminated area of the lamp burner is used separately to obtain the line-of-sight density at that particular position in the lamp burner. This requires that the intensity distribution over the beam stays equal at different wavelengths.

The problems and their solutions that led to the final setup are discussed step by step.

1. *Reference measurement I_0*: The easiest way is to turn the lamp off and then make a wavelength scan (the same scan as the absorption images as described before). But when the lamp is switched on, it heats up and deforms. In this method, the

---

[1]Ideally, one should apply Abel inversion before integrating over the wavelength, because the line shape may vary over the radius of the lamp. However, this is not practical because of noise in the measurement data. By integrating over the line-of-sight the area under curve—and thus the density—might be underestimated by 10–20% (section 2.3).
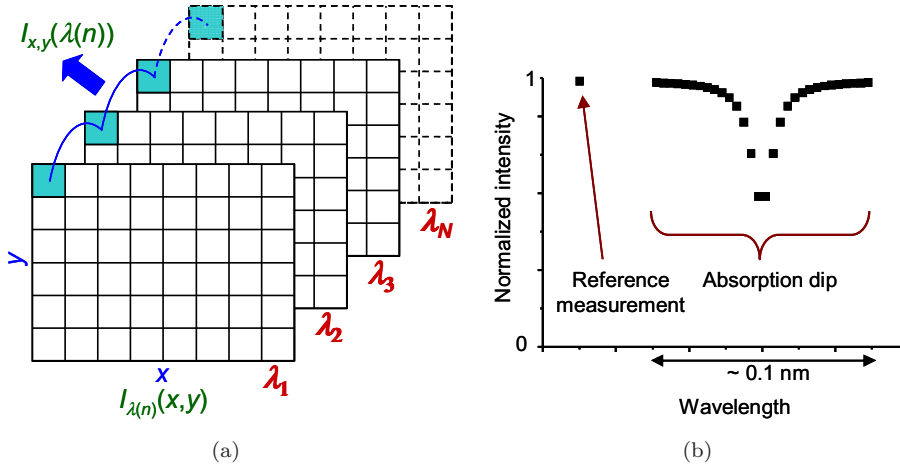
Figure 4.10: Artist impression of the ILAS measurement technique:
(a) For each wavelength λ_n an absorption image $I_{\lambda(n)}(x,y)$ is taken. Next for each pixel (x,y) the absorption dip $I_{x,y}(\lambda(n))$ is constructed.
(b) Impression of the measurement for an arbitrary pixel (x,y) of the CCD camera (not a real measurement). The intensity at the CCD is normalized by dividing the image by the intensity measured by the photodiode. First a reference measurement is taken at a wavelength where no absorption takes place. Next, the actual absorption measurement is performed.

reference measurement is not made under the same conditions as the absorption measurements. By leaving the lamp on and measuring the reference image at a wavelength outside the absorption dip, the same optical conditions as at the absorption measurement images are assured.

2. *Lamp emission I_e*: The light emitted by the lamp is much brighter than the laser light at the CCD (#17; the numbers given in this section refer to the parts in figure 4.11) and therefore it complicates the measurement. To reduce the lamp light on the CCD, an image quality colour filter (#12, LOT-Oriel D640/10m / LOT57900) is used. The transmission for the laser light is ∼80%, whereas the transmission of the lamp light intensity is reduced to ∼1%. The second tool to reduce the lamp light is a diaphragm (#14, diameter 2 mm) in the focal point between the lenses #13 and #15. Because the lamp light is out of focus as compared with the laser light, the diaphragm reduces the lamp light with another factor ∼100. By using both the filter and the diaphragm, the lamp emission intensity is smaller than the laser intensity. The remaining lamp light falling on the CCD is corrected for by subtracting this lamp emission from the
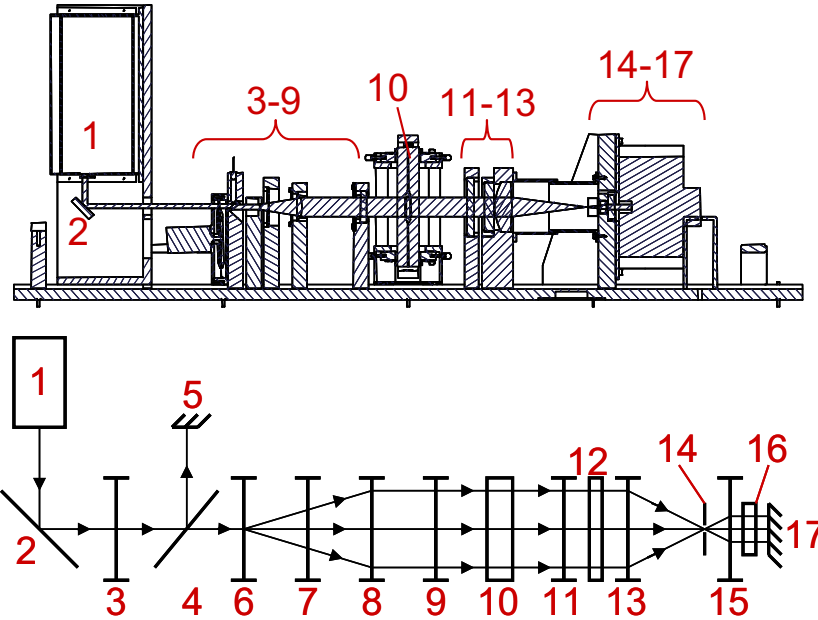
Figure 4.11: Schematic drawing of the ILAS setup: (1) tunable diode laser; (2) mirror (shutter between laser and mirror is not drawn); (3) rotating diffuser; (4) beam splitter; (5) photodiode; (6) spherical lens, $f = -6$ mm; (7) cylindrical lens, $f = -50$ mm; (8) diaphragm and cylindrical lens, $f = 50$ mm; (9) adjustable diaphragm and cylindrical lens, $f = -50$ mm; (10) lamp; (11) cylindrical lens, $f = 100$ mm; (12) colour filter; (13) spherical lens, $f = 80$ mm; (14) adjustable pinhole; (15) spherical lens, $f = 25$ mm; (16) neutral density filter; (17) CCD camera.

measurement images.

3. *Varying laser intensity*: The relative transmission is needed for equation (4.6). For this calculation, the laser intensity before entering the lamp should be independent of the wavelength. The laser intensity, however, is dependent on the wavelength. One has to correct for this effect before comparing measurement images. For this purpose, the intensity values of the images are normalized by dividing those values by the integrated laser intensity ($I_{\mathrm{ph},0}$ and $I_{\mathrm{ph},\lambda}$), which is measured simultaneously by a photodiode (#5). The normalized images are used in the calculations in equation (4.5). For this correction, it is assumed that the laser beam shape is independent of the wavelength and thus the laser light intensity at each position in the beam scales linearly with the total integrated laser intensity measured by the photodiode.
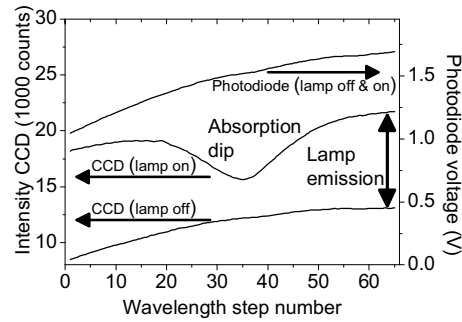
Figure 4.12: Averaged intensity on the CCD chip and photodiode voltage (∼laser intensity) plotted as a function of the wavelength step. The measurements are performed with the lamp off and lamp on. The absorption dip and the lamp emission are indicated.

4. *Laser beam shape dependence of wavelength*: At each CCD pixel a line-of-sight absorption curve is obtained from a small part of the expanded laser beam, this makes the quality of the beam important. But when the laser beam is expanded, a diffraction pattern is observed, which moves when changing the wavelength. This pattern is probably caused by the grating in the laser head. This effect interferes with the spatially resolved absorption measurements, because the assumption that the laser beam shape is independent of the wavelength is no longer valid. To remove this diffraction pattern the laser beam passes a diffuser (#3, POC Light Shaping Diffuser, FWHM angle 0.5°) before entering the lamp. But another problem appears: after passing the diffuser, a speckle pattern shows up. To remove the speckle pattern, the diffuser rotates at 7130 rpm so that the pattern is mixed well and no speckles show up any longer. The value for the shutter time of the CCD camera should be set to at least several times (∼ 10) the rotation time of the diffuser, so that the speckle pattern of the diffuser is averaged out. By using this rotating diffuser, no diffraction pattern is present in the laser beam and the requirement for the beam shape as stated in item 3 is met.

5. *Correlation between the CCD pixel and position in the burner*: The relation between the pixel position on the CCD and the spatial position inside the lamp burner is determined by the optics in the setup. The ray tracing program Zemax [61] is used to calculate the corresponding position in the lamp burner for each CCD pixel. When the corresponding height and lateral coordinates at each CCD pixel are known, a 2D mapping of the ground state atomic Dy density inside the lamp burner is obtained.

Implementing all the described solutions, the ILAS technique gives a 2D lateral particle density distribution inside the plasma volume.
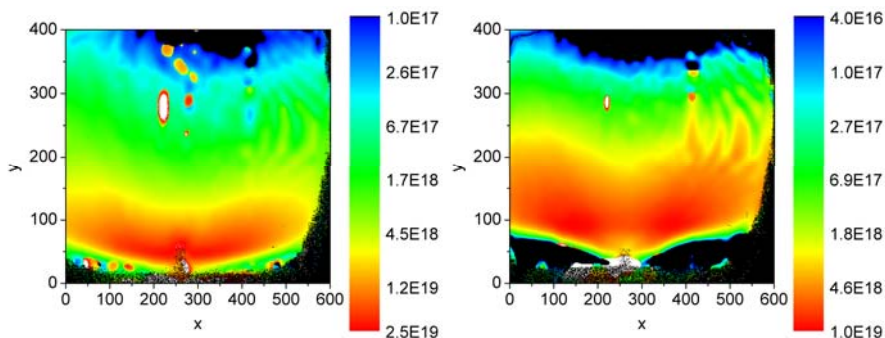
Figure 4.13: Line-of-sight 2D ground state atomic Dy density distribution at (left) 1g and (right) 10g. The coordinates are pixel numbers of the CCD; these are not yet converted to real coordinates inside the burner: $y = 0$ is the bottom and $y = 400$ is the top of the lamp; $x = -140$ and $x = 660$ are approximately the positions of the wall. The Dy density values are given in m^{-2} on a logarithmic scale. Note that the scales of both graphs are different; the density is lower for 10g.

4.4 Results

To prove the ILAS technique in the centrifuge, a measurement on a lamp is presented. Our lamp contains 5 mg Hg, 4 mg DyI$_3$ and 300 mbar Ar/Kr^{85} as a starting gas. The input power is 148 W; the acceleration is 1g and 10g.

Figure 4.12 shows the laser intensity spatially averaged over the lamp (raw data); when the lamp is on and when the lamp is off. In this graph, the absorption dip is clearly seen. Furthermore, the figure shows the photodiode voltage (integrated laser intensity before entering the lamp) that is measured during the wavelength scan. This photodiode voltage is used to normalize the intensity measured by the CCD camera.

After the data (lamp-on condition) have been processed, the 2D ground state atomic Dy density is obtained; this density distribution is shown in figure 4.13. The relation between the lateral pixel number and the real lateral position x is not (completely) linear. Due to the optical system, it is not possible to measure close to the wall. However, we do not expect atomic Dy near the wall because of the lower temperature (section 4.1). The density averaged over the width of the lamp is plotted as a function of the axial position in figure 4.14. It is clearly seen that for 10g, axial segregation is diminished [32, 38]. These graphs show the functioning of the ILAS technique. In the future, Abel inversion will be applied to the line-of-sight 2D density distribution to obtain a 3D cylindrical symmetric ground state atomic Dy density distribution [29, 48, 62–65].
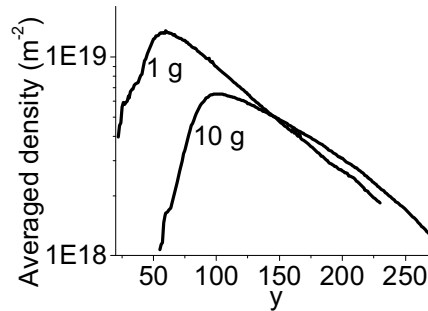
Figure 4.14: Dy density averaged over the width of the lamp (from figure 4.13), for different axial positions y ($y = 0$ is the bottom and $y = 400$ is the top of the lamp). For $10g$ the axial segregation is lower than for $1g$: the density decreases slower towards the top of the lamp for $10g$ than for $1g$. The amount of segregation is g dependent as stated in section 4.1 and figure 4.2. The lower density at the bottom of the lamp is due to electrode effects.

4.5 Conclusions

A new setup has been presented to investigate the metal-halide lamp at hyper-gravity conditions: a centrifuge that allows for the lamp to be accelerated up to $10g$. Higher gravity enhances convection and diminishes axial segregation. The acceleration at the position of the lamp was calibrated, and it was shown that the total acceleration vector was parallel to the lamp axis.

We performed both emission spectroscopy and ILAS on a MH lamp in the centrifuge. With the novel laser absorption measurement technique, a 2D particle density distribution is obtained by taking images of the laser intensity at each wavelength scan step.

First results of the Dy density in a metal-halide lamp were presented to test the ILAS technique under hyper-gravity conditions. This test clearly shows that the setup and measurement techniques are a useful tool to get more insight into the lamp; in this case by measuring the ground state atomic Dy density.

In the future the 2D particle density distribution will be converted to a 3D cylindrical symmetric profile by means of Abel inversion.

Acknowledgements